Laplacian Field of the Effectively Unpaired Electron Density: Determination of Many-Body Effects on Electron Distributions

Rosana M. Lobayan,[†] Roberto C. Bochicchio,*[,‡] Luis Lain,[§] and Alicia Torre[§]

Facultad de Ingeniería, Universidad de la Cuenca del Plata, Lavalle 50, 3400 Corrientes, Argentina, Departamento de Física, Facultad de Ciencias Exactas y Naturales, Universidad de Buenos Aires, Ciudad Universitaria, 1428, Buenos Aires, Argentina, and Departamento de Química Física, Facultad de Ciencias, Universidad del País Vasco, Apdo, 644 E-48080 Bilbao, Spain

Received: November 27, 2006; In Final Form: February 16, 2007

This work carries out the study of the Laplacian field function of the electron density $L(\mathbf{r}) = -\nabla^2\rho(\mathbf{r})$ splitted in two contributions $\rho(\mathbf{r}) = \rho^{(p)}(\mathbf{r}) + \rho^{(u)}(\mathbf{r})$, which correspond to the effectively paired and effectively unpaired electron densities, respectively. The visualization of the concentration and depletion of these fields and their spatial localization show no contribution of the effectively unpaired electrons to the conventional bonding among two centers, but the field $-\nabla^2\rho^{(u)}(\mathbf{r})$ provides an interesting structure. We also study the reliability of the information contained in the partitioning of this electron density field function for describing nonclassical bondings as the three-center two-electron ones.

1. Introduction

The physical interpretation of chemical data is directly related to the extraction of the information contained in the state function of molecular systems, that is generally represented by means of the electron density. There are essentially two treatments of this quantity. On one hand, there are the procedures that integrate the electron density, known as population analyses.[1−3] These procedures count the number of electrons in spatial domains, defined in a determined way, to evaluate classical quantities of chemical interest such as bonding populations (bond multiplicities), atomic populations, valences, free valences, and so forth. These methods will be designated as *nonlocal or integrated formalisms* because they require one to perform an integration of the electron density over the whole real space. The Mulliken-type partitionings[4] are within the most popular population analysis methods; these treatments support the definition of an atom by means of the atomic basis functions centered on each nucleus in the molecule, and consequently, the atomic and bonding regions become automatically defined regarding the localization of these atomic functions.[5−7] The other group of methods adjudicates the atomic domains to spatial regions, as the "fuzzy" atoms descriptions[8−12] or the topological atoms in molecules (AIM) theory.[13−16]

On the other hand, in a alternative manner, there are treatments based on the study of the local topological structure of the electron density, $\rho(\mathbf{r})$, and its associated Laplacian field, $\nabla^2\rho(\mathbf{r})$. These treatments are characterized by the localization and classification of their critical points (cp), that is, maxima, minima, or saddle points. This approach will be called the *local formulation* of the theory. The cp's and the values of the Laplacian of the electron density at these points are of paramount importance to describe the electron distribution in molecular systems.[13,14] These points are classified according to the sign of the three eigenvalues of the Hessian matrix of the density, $\rho(\mathbf{r})$. All of them with a negative sign stand for local maxima, which usually are placed in nuclear posititions and are called nuclear critical points (ncp). Two of them negative and the third one positive correspond to a bond critical point (bcp), meaning a space point in which the concentration of the electron density indicates a bonding interaction between two atoms; the first two eigenvalues correspond to the perpendicular curvature and the third one provides a curvature along the intenuclear axis. In this scenario, a covalent bond is featured by the electron cloud possessing two large negative curvatures perpendicular to the bond line and a small positive curvature along the bond at the position of the bcp.[13,14] The value of the Laplacian field of the electron density at a point $\mathbf{r}$ is the sum of the curvatures along the orthogonal coordinate axes. Its sign indicates whether the electron density is locally depleted (positive) or locally concentrated (negative), and thus it constitutes valuable information to describe the behavior of the density around a local point.[13,14,17]

In a previous work,[18] we partitioned the electron density $\rho(\mathbf{r})$ into two contributions $\rho^{(p)}(\mathbf{r})$ and $\rho^{(u)}(\mathbf{r})$, which correspond to the effectively paired and unpaired electron densities,[19−24] respectively, so that $\rho(\mathbf{r}) = \rho^{(p)}(\mathbf{r}) + \rho^{(u)}(\mathbf{r})$. We described the behavior of both contributions of the electron density and the shift of their ncp and bcp in comparison with those of the total density. These results have allowed us to show that the positions of the ncp's of $\rho^{(p)}(\mathbf{r})$ are very close to the total $\rho(\mathbf{r})$ ones, while the $\rho^{(u)}(\mathbf{r})$ ncp's are also located close to the nuclear positions but out of the bonding region.[18] In this work, we will mainly focus our attention on the effectively unpaired part of the density, in order to quantify its behavior by means of its Laplacian field. For practical reasons, we will use $L(\mathbf{r}) = -\nabla^2\rho(\mathbf{r})$ instead of the Laplacian itself, because the former is positive for density concentration and negative for density depletion. This task will be performed for each contribution, $-\nabla^2\rho^{(p)}(\mathbf{r})$ and $-\nabla^2\rho^{(u)}(\mathbf{r})$. These functions reveal finer details of the structure of the density, providing a physical picture in the understanding of chemical bondings from a many-body physical point of view.

* To whom correspondence should be addressed. Fax: ++54-11-45763357. E-mail address: rboc@df.uba.ar.
[†] Universidad de la Cuenca del Plata.
[‡] Universidad de Buenos Aires.
[§] Universidad del País Vasco.

10.1021/jp0681101 CCC: $37.00
Published on Web 04/03/2007

The organization of this article is as follows. The second section briefly reports the theoretical framework of the partitioning of the electron density and the relationships between the Laplacian fields of its two contributions and the associated topological quantities. The third section describes the computational details of the calculations performed over a set of selected molecules and the discussion of the results. They reveal that both $\rho^{(p)}(\mathbf{r})$ and $\rho^{(u)}(\mathbf{r})$ contibutions present a shell structure and point out the strong physical significance of the $\rho^{(u)}(\mathbf{r})$ field. Finally, the last section is devoted to the concluding remarks.

2. Theoretical Aspects

2.1. Effectively Paired and Unpaired Electron Densities. The electron density $\rho(\mathbf{r})$ in N-electron molecular systems is defined as the diagonal part of the spin-free first-order reduced density matrix (1-RDM)[2,25]

$$\rho(\mathbf{r}) = {}^1D(\mathbf{r}|\mathbf{r}) \tag{1}$$

where ${}^1D(\mathbf{r}|\mathbf{r})$ stands for the 1-RDM in the coordinate representation.[2,25] Its trace (coordinate integration over the whole real space) is the number of electrons in the system, i.e., $\mathrm{tr}({}^1D) = \int \mathrm{d}\mathbf{r}\ {}^1D(\mathbf{r}|\mathbf{r}) = \int \mathrm{d}\mathbf{r}\ \rho(\mathbf{r}) = N$. The density may be decomposed into two terms as[18]

$$\rho(\mathbf{r}) = \rho^{(p)}(\mathbf{r}) + \rho^{(u)}(\mathbf{r}) \tag{2}$$

where $\rho^{(p)}(\mathbf{r})$ and $\rho^{(u)}(\mathbf{r})$ stand for the effectively paired and unpaired density field contributions to the total density $\rho(\mathbf{r})$. Each of them is defined as

$$\rho^{(p)}(\mathbf{r}) = \frac{1}{2}\int \mathrm{d}\mathbf{r}'\ {}^1D(\mathbf{r}|\mathbf{r}')\ {}^1D(\mathbf{r}'|\mathbf{r}) \tag{3}$$

and

$$\rho^{(u)}(\mathbf{r}) = \frac{1}{2}\,u(\mathbf{r}|\mathbf{r}) \tag{4}$$

respectively, where $u(\mathbf{r}|\mathbf{r})$ is the diagonal element of the effectively unpaired density matrix defined by[19−24]

$$u(\mathbf{r}|\mathbf{r}') = 2\ {}^1D(\mathbf{r}|\mathbf{r}') - {}^1D^2(\mathbf{r}|\mathbf{r}') \tag{5}$$

The physical meaning of the effectively paired and unpaired densities stands for the number of paired (opposite spins) and unpaired (far apart) electrons. The unpaired density has two sources; one of them comes from the spin density (only present in nonsinglet states), and the other corresponds to the many-body effects or correlation effects that are supported by the Coulomb interaction between the particles.[15]

2.2. Laplacian Fields of Electron Densities. The topology of the effectively paired and unpaired density fields characterizes the bondings in a molecule and suggests a rigorous revised theoretical version of the electron-pairing classical model. The information contained in these density fields is the localization of their critical points; finer details for such fields are featured as (r, s) where r is the *rank* (number of nonzero eigenvalues of the Hessian matrix) and s the *signature* (sum of the signs of the eigenvalues). Thus, a ncp is denoted as $(3, -3)$ and a bcp as $(3, -1)$. The equation that locates the cp's of the total density is[13]

$$\nabla\rho(\mathbf{r})|_{\mathbf{r}^c} = 0 \tag{6}$$

where $\mathbf{r}^c = \{\mathbf{r}_i^c;\ i = 1, ..., M\}$ stands for the set of critical points of the total density $\rho(\mathbf{r})$, i.e., points in which the total density exhibits a *local* extreme. The Laplacian field of eq 2 yields

$$\nabla^2\rho(\mathbf{r})|_{\mathbf{r}^c} = \nabla^2\rho^{(p)}(\mathbf{r})|_{\mathbf{r}^c} + \nabla^2\rho^{(u)}(\mathbf{r})|_{\mathbf{r}^c} \neq 0 \tag{7}$$

We will use the function $L(\mathbf{r}) = -\nabla^2\rho(\mathbf{r})$ as an indicator of concentration (positive value) or depletion (negative value) of the number of electrons at the point $\mathbf{r}$[26,27] (the terms "accumulation" and "reduction" have been proposed for the description of maxima and minima in $\rho(\mathbf{r})$[17]). According to eq 7, both $\nabla^2\rho^{(p)}(\mathbf{r})|_{\mathbf{r}^c}$ and $\nabla^2\rho^{(u)}(\mathbf{r})|_{\mathbf{r}^c}$ contributions do not necessarily have identical signs in the neighborhood of a $\nabla^2\rho(\mathbf{r})$ cp, and therefore, each of them may concentrate or deplete at that point. It is worthwhile to remark that the results reported in ref 18 have shown the closeness between $\rho^{(p)}(\mathbf{r})$ and $\rho(\mathbf{r})$ so that it is expected that the shell structure of the latter[26] will be transferred to the former one. However, eq 7 does not provide a priori a shell structure for the unpaired density, and thus it deserves to be studied.

3. Computational Details, Results, and Discussion

The state functions for the molecular systems described in the present work were calculated at the level of configuration interaction (CI) with single and double excitations (CISD), using the *Gaussian 03* package[28] with the basis sets 6-31G**. For all systems, the geometries were optimized within this approximation. The densities, their critical points, and their Laplacian fields $\nabla^2\rho^{(p)}(\mathbf{r})$ and $\nabla^2\rho^{(u)}(\mathbf{r})$ were determined by appropriately modified AIMPAC modules.[29] The selected systems have been chosen to cover different types of bondings, that is, molecules with classical patterns (H_2, N_2, HF, NaCl, H_2O, CH_4, C_2H_4) and systems possessing three-center bondings (H_3^+, B_2H_6).

The decomposition of the total electron density $\rho(\mathbf{r})$ into paired $\rho^{(p)}(\mathbf{r})$ and unpaired $\rho^{(u)}(\mathbf{r})$ components allows us to explore each of these fields by means of the Laplacian operator, in order to obtain fine details about the electron distribution. The calculations of this topological description will be shown by means of numerical results as well as by contour maps of both Laplacian fields. The $L(\mathbf{r})$ function values for $\rho^{(p)}(\mathbf{r})$ and $\rho^{(u)}(\mathbf{r})$ at bcp's and ncp's of the total density $\rho(\mathbf{r})$ are shown in Tables 1 and 2, respectively, and the corresponding contour maps are displayed in Figures 1−9. We will discuss the information provided by the Laplacian fields of the densities to determine the extent of concentration or depletion of each density field at the cp's. Then this information will be used to determine and describe the structure of each field.

The results in Table 1 show the behavior of the electron density at the bcp's. As can be seen, $L(\mathbf{r})$ of $\rho^{(p)}(\mathbf{r})$ is greater in absolute value for at least 2 orders of magnitude than $L(\mathbf{r})$ of $\rho^{(u)}(\mathbf{r})$ in all systems except in those possessing three-center two-electron bondings that will be discussed separately. $-\nabla^2\rho^{(p)}(\mathbf{r})$ and $-\nabla^2\rho^{(u)}(\mathbf{r})$ have identical signs in systems possessing an appreciable ionic character as HF, NaCl, and H_2O, while in systems of covalent nature such as CH_4 and C_2H_4, the paired component concentrates and the unpaired depletes. The higher depletion of the unpaired component in the C_2H_4 molecule must be interpreted in terms of the diradical character associated with the double bond in this molecule.[30] The results in Table 2 show a similar behavior of both laplacian fields at ncp's, i.e., both components concentrate for all nuclei irrespective of the nature of the bondings. The contour maps of $L(\mathbf{r})$ for paired and unpaired densities are shown in the figures. Positive (locally concentrated field) and negative (locally depleted field) values

TABLE 1: $L(\mathbf{r})$ of $\rho^{(p)}(\mathbf{r})$ and $\rho^{(u)}(\mathbf{r})$ Densities at Bond Critical Points of $\rho(\mathbf{r})$ at CISD/6-31G Level of Approximation[e]**

system	bond	$-\nabla^2\rho(\mathbf{r})\|_{bcp}$	$-\nabla^2\rho^{(p)}(\mathbf{r})\|_{bcp}$	$-\nabla^2\rho^{(u)}(\mathbf{r})\|_{bcp}$	δ_u[b]
H_2	HH	1.35748	1.35729	0.00019	
N_2	NN	2.24077	2.32333	−0.08256	
HF	FH	2.68565	2.62305	0.06260	
				−0.03404[a]	3.05410^{-1}
NaCl	NaCl	−0.19147	−0.19085	−0.00062	
					c
H_2O	OH	2.10263	2.08116	0.02147	
				−0.02325[a]	2.41910^{-1}
CH_4	CH	0.98670	0.99207	−0.00537	
				−0.00499[a]	1.35110^{-4}
C_2H_4	CC	1.04944	1.06599	−0.01655	
	CH	1.06484	1.07221	−0.00736	
				−0.00645[a]	0.82510^{-2}
H_3^+	HH	0.77714	0.79175	−0.01461	
				0.00006[a]	4.44110^{-1}
B_2H_6	BH(bridge)	−0.145566	−0.155817	0.01025	
				0.00459[a]	5.06210^{-1}
	BH(terminal)	0.24203	0.225876	0.01616	
				0.00376[a]	3.62110^{-1}
	BB[d]	−0.04067	−0.041511	−0.00084	

[a] Laplacian of $\rho^{(u)}(\mathbf{r})$ at its own bond critical point (bcp). [b] Distance between unpaired and total density bcp's. [c] No $\rho^{(u)}(\mathbf{r})$ cp's were found within the topological bonding region. [d] rcp (ring critical point). There is no bcp between boron atoms. [e] All quantities are in atomic units.

TABLE 2: $L(\mathbf{r})$ of $\rho^{(p)}(\mathbf{r})$ and $\rho^{(u)}(\mathbf{r})$ Densities at Nuclear Critical Points of $\rho(\mathbf{r})$ at CISD/6-31G Level of Approximation[b]**

system	nucleus	$-\nabla^2\rho(\mathbf{r})\|_{ncp}$	$-\nabla^2\rho^{(p)}(\mathbf{r})\|_{ncp}$	$-\nabla^2\rho^{(u)}(\mathbf{r})\|_{ncp}$
H_2	H	18.92537	17.94441	0.98095
N_2	N	971548.50321	971020.52592	527.97729
FH	F	3523740.3220	3522356.4205	1383.90157
	H	15.21654	14.49577	0.72077
NaCl	Na	9598280.7879	9598188.6802	92.10771
			9598671.4358[a]	2796.55572[a]
	Cl	91186305.667	91179569.209	6736.4583
			91212299.624[a]	7200.5999[a]
H_2O	O	1921522.4773	1920572.8301	949.64720
	H	17.02506	16.24278	0.78229
CH_4	C	436297.71747	436042.51687	255.20060
	H	19.15135	18.29739	0.85396
C_2H_4	C	436895.28697	436637.02744	258.25953
	H	19.30124	18.54049	0.76075
H_3^+	H	16.06514	15.24387	0.82127
B_2H_6	B	168831.76379	168741.28402	90.47977
	H (bridge)	19.80936	18.95469	0.85467
	H (terminal)	18.81488	18.04548	0.76940

[a] Value for isolated atom. [b] All quantities are in atomic units.

in the contour maps are denoted by solid and dashed lines, respectively.

Figures 1−7 show the contour maps for the H_2, N_2, HF, H_2O, CH_4, C_2H_4 and NaCl molecules, respectively. All of them show that the paired component is concentrated at the nuclear regions and at the bonding regions (those lying in the interatomic part of the space joining the nuclei and possessing a bcp) except the NaCl system (cf. Figure 7). This molecule exhibits a completely depleted paired field in its bonding region, which gives rise to a high concentration at the nuclei; this result reflects the well-known strong ionic character of this molecule. The unpaired component instead always appears concentrated at the nucleus zones showing an appreciable depletion in most of cases at the bonding regions. In the H_2, HF, and H_2O molecules, the unpaired component decreases less than in the other systems: this is due to the spatial extension of this density from the nuclear positions toward the bonding regions, which may be seen in the contour maps. In the H_2 system (cf. Table 1 and

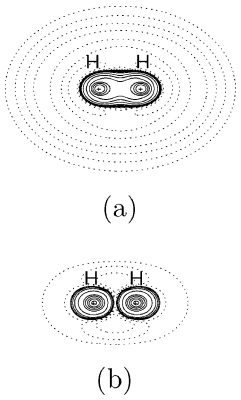

Figure 1. $L(\mathbf{r})$ contour maps of H_2 molecule for effectively paired ((a)) and effectively unpaired densities ((b)). Positive and negative values are denoted by solid and dashed lines, respectively.

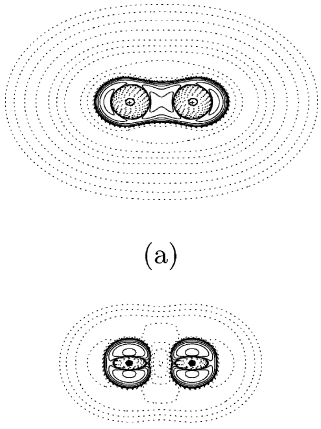

Figure 2. $L(\mathbf{r})$ contour maps of N_2 molecule for effectively paired ((a)) and effectively unpaired densities ((b)). Positive and negative values are denoted by solid and dashed lines, respectively.

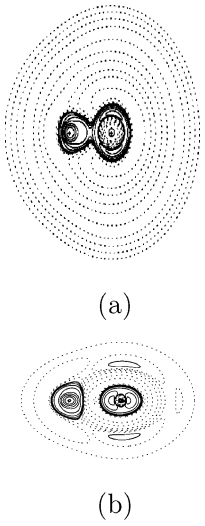

Figure 3. $L(\mathbf{r})$ contour maps of HF molecule for effectively paired ((a)) and effectively unpaired densities ((b)). Positive and negative values are denoted by solid and dashed lines, respectively.

Figure 1), the concentration of the unpaired component is centered at the nucleus positions, and it is also extended over a large zone containing the bonding region, as can be observed on the contour maps. This fact is in agreement with its easy attack by other species. The behavior of the unpaired field in the HF and H_2O molecules may be interpreted as an indicator

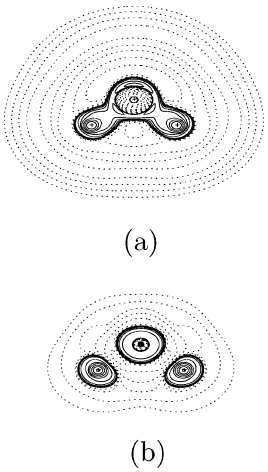

Figure 4. $L(\mathbf{r})$ contour maps of H_2O molecule for effectively paired ((a)) and effectively unpaired densities ((b)). Positive and negative values are denoted by solid and dashed lines, respectively.

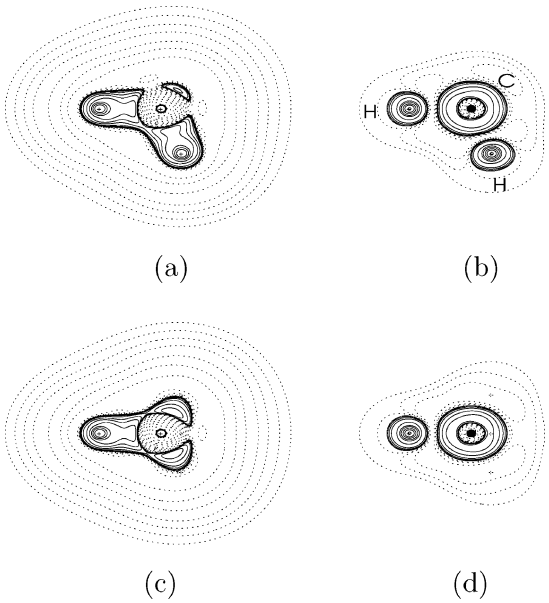

Figure 5. $L(\mathbf{r})$ contour maps of CH_4 molecule for effectively paired ((a)) and effectively unpaired densities ((b)). Positive and negative values are denoted by solid and dashed lines, respectively. In (a) and (b), the fields are shown in the plane containing the CH bonds; in (c) and (d), the contour maps correspond to a plane perpendicular to the previous one.

of the ionic character of their bonds (cf. Table 1 and Figures 3 and 4). All these systems possess two-center two-electron bonds so that these results may be interpreted as features of this kind of bonding. As has been shown, $\nabla^2\rho^{(u)}(\mathbf{r})$ depletes (or it is very small) and $\nabla^2\rho(\mathbf{r})$ and $\nabla^2\rho^{(p)}(\mathbf{r})$ concentrate at bcp's of $\rho(\mathbf{r})$ for two-center bondings of covalent nature. However, the polarity of the bonding may change the sign of these fields, although $\nabla^2\rho^{(u)}(\mathbf{r})$ depletes at $\rho^{(u)}(\mathbf{r})$ bcp's in these cases. These results are in agreement with those obtained in previous works[16,18] in the study of the electron density $\rho(\mathbf{r})$ for these systems.

A survey in Figures 1−7 permits us to draw out features common to all studied systems. The continued-line central circles (concentration region) and its neighboring dashed-line ones (depletion region) constitute shells. This fact means that both fields possess concentration of charge just over the nucleus positions and then present a depletion around that nuclear concentration. This is an expected result for the paired density, which is very close to the total density. However, it is

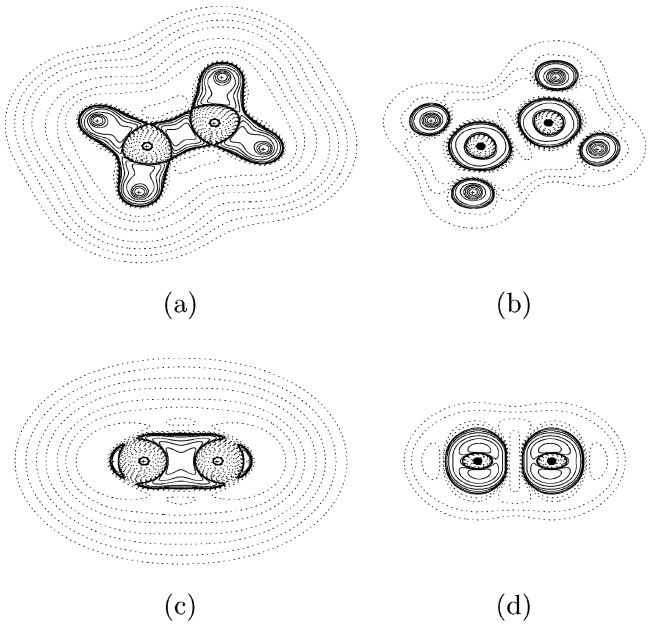

Figure 6. $L(\mathbf{r})$ contour maps of C_2H_4 molecule for effectively paired ((a)) and effectively unpaired densities ((b)). Positive and negative values are denoted by solid and dashed lines, respectively. In (a) and (b), the fields are shown in the plane containing the CH bonds; in (c) and (d), the contour maps correspond to a plane perpendicular to the previous one.

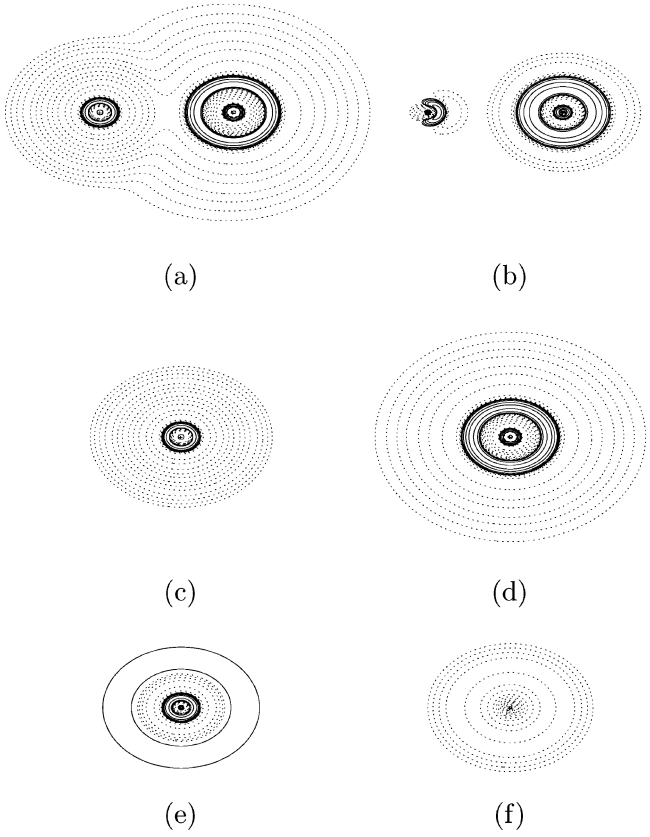

Figure 7. $L(\mathbf{r})$ contour maps of NaCl molecule for effectively paired ((a)) and effectively unpaired densities ((b)). Positive and negative values are denoted by solid and dashed lines, respectively; (c) and (d) are the contour maps of the effectively paired and unpaired components of Na, and (e) and (f) are the contour maps of the effectively paired and unpaired components of Cl free atoms, respectively.

unexpected for the unpaired component, which is very small in comparison with the paired one. Thus, the unpaired density also

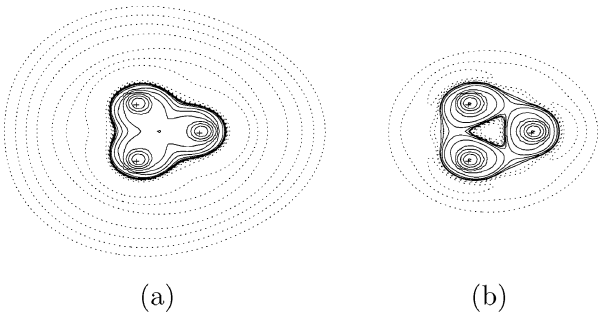

Figure 8. $L(\mathbf{r})$ contour maps of H_3^+ molecule for effectively paired (a) and effectively unpaired densities (b). Positive and negative values are denoted by solid and dashed lines, respectively, in the contour maps.

has a shell structure. We will characterize the shell structures of both components defining regions that will be called according to the scheme followed in ref 26 for the total density, that is, the inner regions define the core shell of paired charge concentration (CSPCC), the core shell of paired charge depletion (CSPCD), the core shell of unpaired charge concentration (CSUCC), and the core shell of unpaired charge depletion (CSUCD). The core shell of charge depletion for any of the fields ends at the lines in which the field shows another outer space region of concentration (continued lines). These shells of paired and unpaired charge concentration will be called valence shell of paired charge concentration (VSPCC) and valence shell of unpaired charge concentration (VSUCC), respectively. The VSPCCs are placed around each nucleus and extended over the bonding zone, while VSUCCs instead are only placed around each nucleus. The outer dashed lines which follow the VSCCs are called valence shell of paired or unpaired charge depletion (VSPCD) and (VSUCD), respectively. Note that, in the spatial region in which VSUCC shows higher concentration, the VSPCC exhibits lower concentration and there are also regions in which both fields deplete.

The contour maps for CH_4 and C_2H_4 molecules are displayed in Figures 5 and 6. In versions (a) and (b) of these figures, the fields are shown in a plane containing a CH_2 group, while in the (c) and (d) versions, the contour maps correspond to a plane perpendicular to the previous one, containing only one CH bond. The contour maps show that the VSPCC is distributed over the CH and CC bonds. The VSUCC preserves a high spherical symmetry which indicates the atomic character of this density. For the C_2H_4 system, a slight distortion of this spherical symmetry may be noted in the plane perpendicular to the molecular plane (Figure 6b). This fact is related to the formation of a double bond of π nature showing the unpaired density delocalized over the bonding region; consequently, this feature of the VSUCC is similar to that observed in the N_2 system (cf. Figure 2). The contour maps for the NaCl molecule are shown in Figure 7 as well as the isolated atomic contour maps for both densities. This system has been chosen as a conventional example of pure ionic character to show the behavior of the fields in this kind of molecule. The chlorine atom in the NaCl molecule (Figure 7a,b) presents three well-defined regions of concentration/depletion of the density: a core, an intermediate region, and a valence shell for both density fields. The VSPCC is not widespread over the bonding zone, and consequently, it is close to the VSUCC, i.e., both VS are localized around each nucleus due to the ionic character of the bonding among sodium and chlorine atoms. Figure 7c−f shows the contour maps for

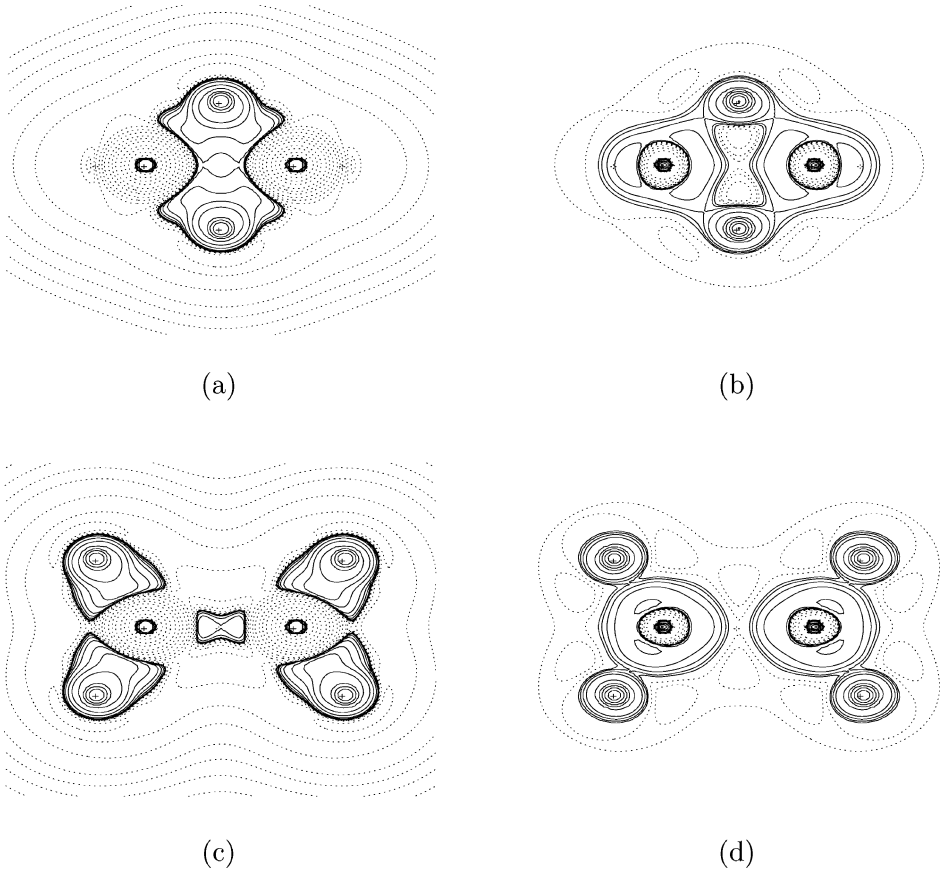

Figure 9. $L(\mathbf{r})$ contour maps of B_2H_6 molecule for effectively paired (a) and effectively unpaired densities (b). Positive and negative values are denoted by solid and dashed lines, respectively, in the contour maps. In (a) and (b), the fields are shown in the plane containing the bridge atoms and the ring critical point; in (c) and (d), the contour maps correspond to the plane perpendicular to the previous one in which the BeH_2 groups lie.

the isolated atoms. The isolated chlorine atom presents a typical pattern for the paired distribution which is very close to the corresponding atom in the molecular environment. The paired electron cloud is localized in space showing well-defined electronic quantum shells. However, for the unpaired distribution, we have found neither shells nor concentrations (absence of continuous lines), because the shells are almost complete and consequently the unpaired Laplacian density component is negligible. The isolated Na atom presents two shells of paired concentration and three shells of unpaired concentration. Therefore, the paired electrons are localized in the real space within the complete inner shells of Na and VSPCC is not found, because there is only one electron, which cannot be paired, in the valence shell. These results show that the differences between the densities of the isolated atoms and the densities of these atoms within the molecular environment are more drastic for the unpaired component. The contour maps of the unpaired distribution show that the Na atom immersed in the NaCl bonding loses its unpaired electron and then its spherical symmetry becomes distorted. This picture is clearly interpreted as the M-shell is polarized to the direction of the Cl atom. The bonded Cl atom is attached to the Na outer unpaired electron, and consequently, the unpaired density in its internal shells become increased, showing zones of concentration. Thus, the unpaired distribution appears strongly modified in the molecular framework of bond formation, while the paired atomic distribution remains almost unaltered.

The above-described contour map features provide interesting information from the results collected in Table 1 concerning the covalent or ionic character of the bondings. In the N_2, CH_4, and C_2H_4 molecules, $\nabla^2\rho^{(p)}(\mathbf{r})$ concentrates while $\nabla\ ^2\rho^{(u)}(\mathbf{r})$ depletes even at its own bcp. However, the molecules possessing a strong ionic character, such as HF and H_2O, show the opposite behavior, and both Laplacian components have identical signs at the bcp's of $\rho(\mathbf{r})$. These results seem to be a consequence of the negligible distance between $\rho(\mathbf{r})$ and $\rho^{(u)}(\mathbf{r})$ bcp's. Regarding the two above-mentioned systems with appreciable ionic character in their bonds, both components concentrate at $\rho(\mathbf{r})$ bcp's but the unpaired component depletes at its own bcp's. It may be noted that in this case the shift of both ccp's is not negligible.

The last two systems, H_3^+ and B_2H_6, are typical examples of electron-deficient molecules possessing three-center two-electron bondings.[31] These systems, which have been widely studied by means of integrated formalisms, are interesting to test our methodology beyond the more conventional type of bondings. The behavior of both paired and unpaired density Laplacian components is useful to note new features for these types of electron distributions. The information related with these systems can be observed in Tables 1 and 2 and Figures 8 and 9. As is well-known, the H_3^+ ion presents three bcp's, but they do not lie in the line joining two nuclei but are rather displaced toward the center of gravity of the system in which a ring critical point (rcp) appears.[13,14] The Laplacian of the paired density concentrates at the bcp, while the unpaired one depletes, showing a behavior similar to that of the covalent type of bonding discussed above. However, the unpaired component concentrates at its own bcp, although its value is practically zero. Figure 9 shows that both Laplacian density components are concentrated around the nuclei with a great delocalization of the unpaired one surrounding the central ring zone but appreciably depleted at the ring critical point on which only the paired component concentrates. The behavior of the B_2H_6 system is more complex. The bcp's are placed in the BH bonding regions of both BH_2 terminal groups and those forming the bridge. No bcp exists between boron atoms, but a ring critical point appears in the BB interatomic line. The values in Table 1 show a paired component depletion at the BH (bridge) and a concentration at the BH (terminal), while the unpaired component concentrates at both BHs. These results allow us to interpret that the deficiency of electrons induces a greater delocalization of the unpaired density. These facts may be observed in Figure 9a,b for a plane containing the bridge H atoms and in Figure 9c,d for the plane in which the BH_2 groups lie. The values in Table 2 are easily interpreted, because both fields present accumulation at the nuclear positions as expected.

4. Final Remarks and Conclusions

In this work, we have studied the electron distribution behavior in molecular systems. This study is based on the mathematical partitioning of the electron density $\rho(\mathbf{r})$ into two contributions of different nature, the effectively paired density $\rho^{(p)}(\mathbf{r})$ and the effectively unpaired one $\rho^{(u)}(\mathbf{r})$. This procedure preserves the conventional chemical bonding concept, i.e., only paired electrons may contribute to constitute a chemical bond, which has been shown here using the Laplacian functions of both density fields. The paired part of the density is mainly localized in bonding and nuclear regions, while the unpaired one is only near the nuclear positions. Nuclear regions possess the greatest portion of effectively unpaired electrons. It has been shown that the paired as well as the unpaired densities possess a shell structure. This fact is not surprissing for the paired density because it is close to the total density. However, the shell structure found with successive regions of concentration and depletion of the unpaired density is an important result. The shell structures of both components are similar to what is known for the total density, and thus the spatial zones may be classified in the same way: core shell of paired and unpaired charge concentration, core shell of paired and unpaired charge depletion, valence shell of paired and unpaired charge concentration, and valence shell of paired and unpaired charge depletion. The features of both fields may be seen clearly in systems with conventional two-center patterns, ranging from systems with covalent bondings to those having an appreciable ionic character. The concentration and depletion of each Laplacian density component around its bond critical points reveal some details of its neighborhood and the pure ionic limit. Systems possessing three-center two-electron bonding patterns have also been described showing the reliability of the information obtained throughout this density description. It is also worthwhile to note as a final remark that this methodology can be applied to any correlated level of the theory, because only the occupation numbers and their associated eigenvectors are needed to evaluate the density or any other function of it (i.e., the Laplacian density in this case) and to extract the critical points for such fields.

Acknowledgment. R.M.L. acknowledges aid from Universidad de la Cuenca del Plata (Corrientes, Argentina) for facilities provided during the course of this work. R.C.B. acknowledges grants in aid from the Universidad de Buenos Aires (project no. X-024) and the Consejo Nacional de Investigaciones Científicas y Técnicas, República Argentina (PIP no. 5098/05), and the Department of Physics, Facultad de Ciencias Exactas y Naturales, Universidad de Buenos Aires, for facilities provided during the course of this work. L. L. and A. T. acknowledge grants from Spanish Ministry of Education (grant no. CTQ2006-01849/BQU) and Universidad del Pais Vasco (grant no. GIU06/03).

References and Notes

(1) McWeeny, R. *Methods of Molecular Quantum Mechanics*; Academic: London, 1969; see also references therein.

(2) Davidson, E. R. *Reduced Density Matrices in Quantum Chemistry*; Academic: New York, 1976; see also references therein.

(3) Szabo, A.; Ostlund, N. S. *Modern Quantum Chemistry: Introduction to Advanced Electronic Structure*; Macmillan Publishing Co.: New York, 1982.

(4) Mulliken, M. S. *J. Chem. Phys.* **1955**, *23*, 1833.

(5) Robby, K. *Mol. Phys.* **1974**, *27*, 81.

(6) Wiberg, K. *Tetrahedron* **1968**, *24*, 1083.

(7) Bochicchio, R. C. *THEOCHEM* **1991**, *228*, 209.

(8) Salvador, P.; Mayer, I. *J. Chem. Phys.* **2004**, *120*, 5046.

(9) Hirshfeld, F. L. *Theor. Chim. Acta* **1977**, *44*, 129.

(10) Davidson, E. R.; Chakravorty, S. *Theor. Chim. Acta* **1992**, *44*, 129.

(11) Alcoba, D. R.; Torre, A.; Lain, L.; Bochicchio, R. C. *J. Chem. Phys.* **2005**, *122*, 74102.

(12) Torre, A.; Alcoba, D. R.; Lain, L.; Bochicchio, R. C. *J. Phys. Chem. A* **2005**, *109*, 6587.

(13) Bader, R. F. W. *Atoms in Molecules: A Quantum Theory*; Clarendon Press: Oxford, U.K., 1994; see also references therein.

(14) Popelier, P. L. A. *Atoms in Molecules: An Introduction*; Pearson Education: London, 1999.

(15) Torre, A.; Lain, L.; Bochicchio, R. C. *J. Phys. Chem. A* **2003**, *107*, 127.

(16) (a) Bochicchio, R. C.; Lain, L.; Torre, A. *Chem. Phys. Lett.* **2003**, *374*, 576. (b) Bochicchio, R. C.; Lain, L.; Torre, A. *Chem. Phys. Lett.* **2003**, *375*, 45.

(17) Bader, R. F. W. *Chem.—Eur. J.* **2006**, *12*, 7769.

(18) Lobayan, R. M.; Bochicchio, R. C.; Lain, L.; Torre, A. *J. Chem. Phys.* **2005**, *123*, 144116.

(19) Takatsuka, K.; Fueno, Yamaguchi, K. *Theor. Chim. Acta* **1978**, *48*, 175.

(20) Takatsuka, K.; T. Fueno, T. *J. Chem. Phys.* **1978**, *69*, 661.

(21) Bochicchio, R. C. *THEOCHEM* **1998**, *429*, 229.

(22) Staroverov, V. N.; Davidson, E. R. *Chem. Phys. Lett.* **2000**, *330*, 161.

(23) Lain, L.; Torre, A.; Bochicchio, R. C.; Ponec, R. *Chem. Phys. Lett.* **2001**, *346*, 283.

(24) Alcoba, D. R.; Bochicchio, R. C.; Lain, L.; Torre, A. *Chem. Phys. Lett.* **2006**, *429*, 286.

(25) Coleman A. J.; Yukalov V. I. *Reduced Density Matrices: Coulson's Challange*; Lecture Notes in Chemistry, Vol. 72; Springer: Berlin, 2000.

(26) Popelier, P. L. A. *Coord. Chem. Rev.* **2000**, *197*, 169.

(27) Guillespie, R. J.; Popelier, P. L. A. *Chemical Bonding and Geometry*; Oxford University Publishers: New York, 2001.

(28) Frisch, M. J.; Trucks, G. W.; Schlegel, H. B.; Scuseria, G. E.; Robb, M. A.; Cheeseman, J. R.; Montgomery, J. A., Jr.; Vreven, T.; Kudin, K. N.; Burant, J. C.; Millam, J. M; Iyengar, S. S.; Tomasi, J.; Barone, V.; Mennucci, B.; Cossi, M.; Scalmani, G.; Rega, N.; Petersson, G. A.; Nakatsuji, H.; Hada, M.; Ehara, M.; Toyota, K.; Fukuda, R.; Hasegawa, J.; Ishida, M.; Nakajima, T.; Honda, Y.; Kitao, O.; Nakai, H.; Klene, M.; Li, X.; Knox, J. E.; Hratchian, H. P.; Cross, J. B.; Adamo, C.; Jaramillo, J.; Gomperts, R.; Stratmann, R. E.; Yazyev, O.; Austin, A. J.; Cammi, R.; Pomelli, C.; Ochterski, J. W.; Ayala, P. Y.; Morokuma, K.; Voth, G. A.; Salvador, P.; Dannenberg, J. J.; Zakrzewski, V. G.; Dapprich, S.; Daniels, A. D.; Strain, M. C.; Farkas, O.; Malick, D. K.; Rabuck, A. D.; Raghavachari, K.; Foresman, J. B.; Ortiz, J. V.; Cui, Q.; Baboul, A. G.; Clifford, S.; Cioslowski, J.; Stefanov, B. B.; Liu, G.; Liashenko, A.; Piskorz, P.; Komaromi, I.; Martin, R. L.; Fox, D. J.; Keith, T.; Al-Laham, M. A.; Peng, C. Y.; Nanayakkara, A.; Challacombe, M.; Gill, P. M. W.; Johnson, B.; Chen, W.; Wong, M. W.; C. Gonzalez, C.; Pople, J. A. *Gaussian 03*, revision C.02; Gaussian, Inc.: Wallingford, CT, 2004.

(29) Biegler-Köning, F. W.; Bader, R. F. W.; Tang, T. H. *J. Comput. Chem.* **1982**, *13*, 317.

(30) Medrano, J. A.; Reale, H. F. *THEOCHEM* **1985**, *121*, 259.

(31) Wade, K. *Electron Deficient Compounds. Studies in Modern Chemistry*; Nelson and Sons, Ltd.: 1971.